Cell aggregation: Packing soft grains

J. A. Åström[1] and M. Karttunen[2,*]
[1]*Centre for Scientific Computing, P.O. Box 405 FIN-02101 Esbo, Finland*
[2]*Biophysics and Statistical Mechanics Group, Laboratory of Computational Engineering, Helsinki University of Technology, P.O. Box 9203, FIN-02015 HUT, Finland*
(Received 16 March 2005; published 7 June 2006)

Cellular aggregates may be considered as collections of membrane enclosed units with a pressure difference between the internal and external liquid phases. Cells are kept together by membrane adhesion and/or confined space compression. Pattern formation and, in particular, intercellular spacing have important roles in controlling solvent diffusion within such aggregates. A physical approach is used to study generic aspects of cellular packings in a confined space. Average material properties are derived from the free energy. The appearance of penetrating intercellular void channels is found to be critically governed by the cell wall adhesion mechanisms during the formation of dense aggregates. A fully relaxed aggregate efficiently hinders solvent diffusion at high hydrostatic pressures, while a small fraction (~ 0.1) of adhesion related packing frustration is sufficient for breaking such a blockage even at high a pressure.

DOI: 10.1103/PhysRevE.73.062301 PACS number(s): 45.70.−n, 62.40.+i, 83.80.Hj

Broadly defined, granular materials include all materials which are divided into discrete cells on a scale significantly larger than the atomic one. They include, e.g., all porous materials, emulsions, foams, with one or several characteristic length scale for the pores, and all living matter. From the statistical physics point of view the first three have received a lot of attention in the context of granular matter, while the last one, the living matter, has so far been largely neglected.

During its initial stages of existence, multicellular organisms grow by generating cellular aggregates. Such aggregates may grow in a way that minimize surface area if adhesion is strong [1]. In a confined geometry dense aggregates may form as a result of internal pressure, irrespective of adhesion. The ultimate porosity and coordination number, and their fluctuations within such an emerging structure, will affect, e.g., the permeability of solutes to the cells from the surrounding solution. This may apply to growing tumors [2] and is of particular importance in the nutrient uptake of plants [3,4].

A cellular aggregate consists of discrete solid and deformable membranes with a pressure difference between internal and external liquid phases. In physical terms, this type of system is a hybrid of a foam and solid granular matter. The differences lie mainly in the physical state of the matter forming the grains. Solid granular matter consists of solid grains with a liquid phase in between grains. The "grains" in foams are liquid with a solid or liquid phase separating cells.

The texture of a liquid foam is governed by surface tension and the degree of drainage. A wet aqueous foam has low porosity and no elastic rigidity. A dry foam has a high density of bubbles (i.e., a high porosity) which are interlocked, or jammed, such that they cannot flow past each other [5]. This leads to nonzero bulk and shear stiffness determined by internal compressibility and surface tension. In cellular aggregates the surface tension has no counterpart and, in contrast to cellular aggregates, aqueous foams tend to coarsen with time.

Similar to aqueous foams, the stiffness of a solid granular material is zero below the jamming transition. At the jamming transition the distribution of contact forces is broad (i.e., exponential) and a complex network of force chains appears [6,7]. When pressure is increased beyond the jamming threshold, the deformations of the grains increase and local rearrangements occur. The force chain network then becomes denser and the distribution of the contact forces narrower. Eventually, the exponential distribution should transform into a Gaussian-like distribution [8–10]. Typically, the porosity, and thus the permeability, remains high in a packing of solid grains [11] in contrast to a packing of soft grains. The transformation in the distribution of contact forces is difficult to investigate numerically as there is no easy way to efficiently model large deformations of solid grains. Commonly, Hertz contact forces are applied in numerical simulation models [11,12]. Here, cellular aggregates provide a possibility to model arbitrary large deformations. This motivates the use of the term soft grains.

It is thus clear that soft grains form their own class of granular materials. As will be demonstrated, the average mechanical behavior of soft aggregates can in general be derived from the free energy and there is little difference between low and high friction membranes. In contrast, the fluctuations of the contact forces differ qualitatively. A high friction aggregate can never become compact, thereby leaving relatively open paths for, e.g., nutrient diffusion through the packing even at a high hydrostatic pressure. In the opposite case, a low friction aggregate rapidly becomes compact with increasing pressure, thus efficiently closing all paths.

In our numerical model, cell membranes are modeled as closed loops of spring-mass chains [13]. The equations of motion for a membrane of mass points connected by linear elastic springs (i.e., a minimal model of a single polymer loop) can be written as

$$m\ddot{\vec{\mu}}_i = \sigma_i \vec{\eta}_i - \sigma_{i+1}\vec{\eta}_{i+1} + P(l_0/2)\vec{\nu}_i + P(l_0/2)\vec{\nu}_{i+1}, \qquad (1)$$

where m is the mass of the points i located at $\vec{\mu}_i$, and connected by springs with tension forces σ_i. P is the inflation pressure and l_0 is the length of the unstretched springs. $\vec{\eta}_i$ is a unit vector along spring i, and $\vec{\nu}_i$ is the outward directed

*Present address: Department of Applied Mathematics, The University of Western Ontario, London (ON), Canada.

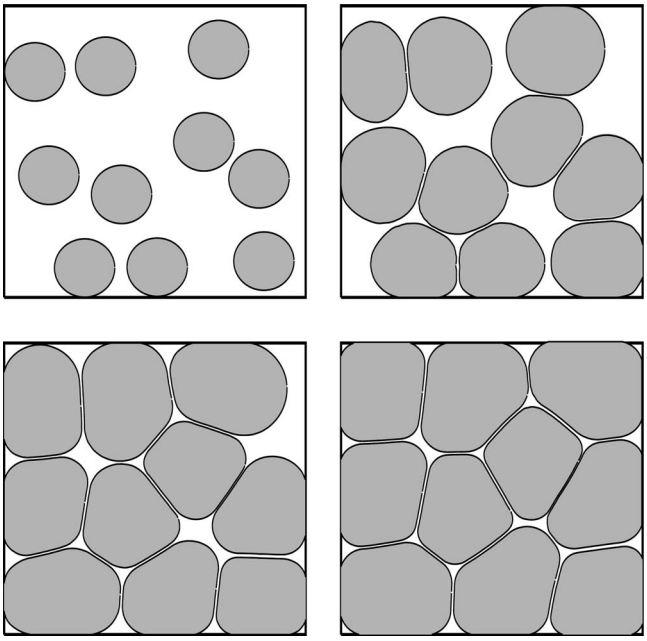

FIG. 1. An aggregate of closed inflated membranes in an elastic box. Friction between membranes is large. The snapshots are taken at pressure forces $Pl=5,10,20,40$.

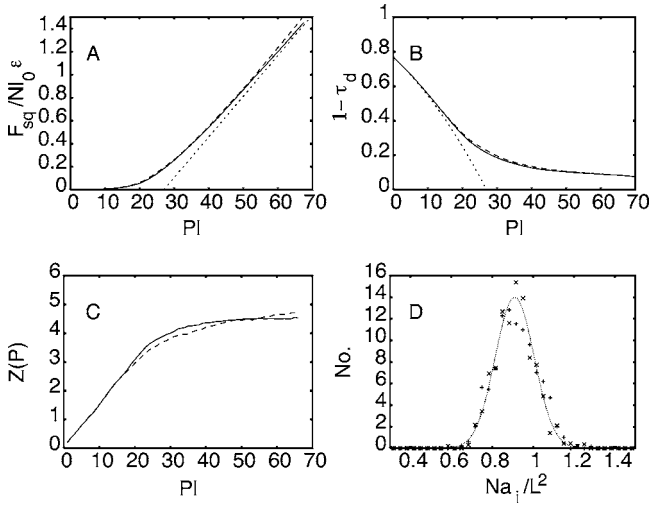

FIG. 2. (a) F_w as a function of Pl_0. The dotted line is the free energy estimate of F_w at low porosity. (b) The porosities $1-\tau$ as functions of Pl_0. The dotted line is the free energy estimate of the porosity at high porosity. (c) $Z(P)$ as function of Pl_0. (d) The distribution of membrane surfaces Na_i/L^2 at $P=50$. (×) frictional packings, (+) zero friction packings. Broken lines represent frictional packings and full lines represent zero friction packings in (a)–(c).

orthogonal unit vector for the same spring. We set the pressure P to be independent of the area inside the membrane (e.g., like a osmotic pressure).

Aggregates are formed by slowly increasing the pressure difference for a set of membranes confined within a two-dimensional box with stiff boundaries. A very stiff short-range harmonic potential between the mass points belonging to different membranes is implemented in order to prevent membranes from penetrating each other (the range of this potential is approximately that of the distance between mass points). We focus on two cases: (I) There is a central force potential around each mass point, i.e., the membranes are prevented from sliding on each other as a result of interlocking ("high" friction). (II) The potential has only a nonzero component orthogonal to the membrane surface meaning that the membranes can freely slide on each other. Snapshots of a small packing of type (I) at different inflation pressures are shown in Fig. 1. An animation of a packing inflation is also available [17].

Our simulation results are because of computational reasons limited to rather small systems. Before analyzing the simulation results we therefore give an analytical description of the force distributions inside a packing starting from the free energy. The free energy does not contain any connection to the finite size of the box used in the simulations and should therefore be valid in the "thermodynamic limit." The temperature is set to zero, which means that the free energy does not contain an entropy term. The equlibrium condition for the free energy is then reduces to a force balance equation.

Let N be the number of membranes contained within a two-dimensional box of size L^2 having stiff boundaries. Each membrane consists of n mass points of mass m connected by n springs with spring constant ϵ. A pressure P is used to inflate each membrane, which means that a pressure force Pl pushes each mass point in the outward direction. The spring length is denoted by l. The free energy F of a circular membrane as a function of its radius r can be written as

$$F = nPl(r_0 - r) + n\epsilon l_0 r_0 \sin\left(\frac{\pi}{n}\right)\left(\frac{r-r_0}{r_0}\right)^2, \tag{2}$$

where r_0 is the equilibrium radius at $P=0$ and $l=l_0$ at $P=0$. The first term is the work done by the inflation pressure, while the second term is the radial component of the elastic energy stored in the springs. Differentiating with respect to r gives the force on a isolated membrane as a function of P and r as

$$f(P,r) = n2\epsilon l_0 \sin\left(\frac{\pi}{n}\right)\left(\frac{r-r_0}{r_0}\right) - nPl. \tag{3}$$

Thus, there is force balance between the stretched membrane and the inflation pressure P, when $r \equiv r_e = r_0 + Plr_0/[2\epsilon l_0 \sin(\frac{\pi}{n})]$. The space filling factor τ of the membranes before the contact formation starts is thus $\tau_d = (N\pi r_e^2)/L^2$. The corresponding porosity $(1-\tau_d)$ goes to zero at $P_\tau l r_0 = 2\epsilon l_0 \sin(\frac{\pi}{n})(\frac{L}{\sqrt{N\pi}} - r_0)$.

Ideally, the membranes in a packing would rearrange themselves into the most optimal configuration (i.e., a hexagonal lattice) as P is increased and the membranes begin to push on each other. A hexagonal lattice will not quite be formed as can be seen, e.g., in the small system in Fig. 1. In particular, at the boundaries of the system the membranes are forced to arrange themselves beside each other along the walls, but there is also "frozen in" disorder in the bulk. As the membranes are pressed flat against the wall at high pressures, it is easy to estimate the total force on the walls, F_w. If the membranes would arrange themselves as a square lattice the force on the walls would be $F_{sq} = P \ln_w$, where $n_w \approx \sqrt{Nn}[1-(P_\tau l)/Pl]$.

F_{sq} and the space filling factor τ_d are compared to simu-

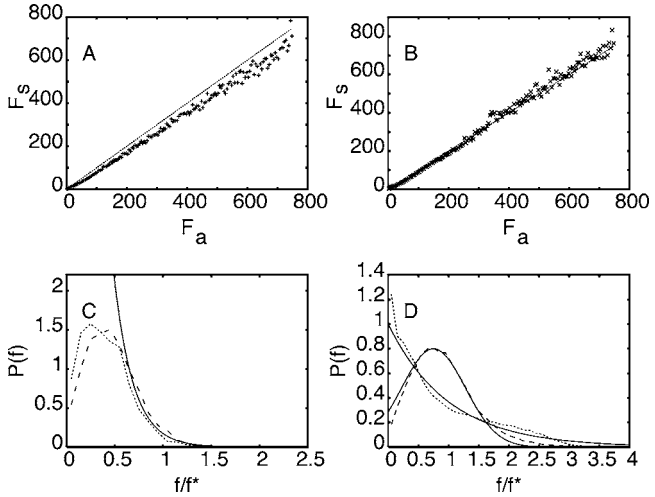

FIG. 3. The average of the contact forces on a membrane. Simulated results F_s are compared to Eq. (3), F_a. (a) High friction. (b) Zero friction. The broken line is $F_s=F_a$. (c) The fluctuation of the contact forces [probability distribution $P(f)$] on a membrane at $Z(P)\approx 2$. The dotted line is for high friction and the broken line for zero friction. The full line is an exponentially decaying function. (d) The fluctuation of the contact forces on a membrane at $Z(P)\approx 4.5$. The distribution for high friction (dotted line) is compared to $P(f) \propto \exp(-f/f^*)$ (full line), and the distribution for zero friction (broken line) is compared to a Gaussian distribution (full line).

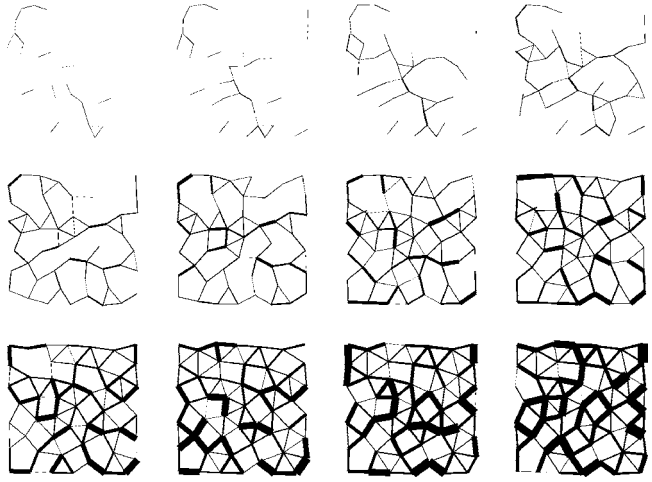

FIG. 4. Force chain network in a small packing with high friction, $N=50$, at $Pl_0=5,10,15,\ldots,60$ from top left to bottom right. Notice percolation at $Pl_0=15$.

lation results in Figs. 2(a) and 2(b), respectively, for packings with $N=50$. As P is increased, the packing undergoes a change from a dilute state in which $\tau\approx\tau_d$ and $F_w\approx 0$ to a dense state in which $F_w\approx F_{sq}$ and $\tau\approx 0$. A transition region between the two states is entered at $Pl_0\approx 15$. This should be compared to the average coordination number, $Z(P)$, in Fig. 2(c). The transition region is entered when $Z\approx 2$, which is roughly the point at which membranes in contact percolate. This is in contrast to frictionless solid grains for which the jamming transition, and thereby non-zero forces, appear at $Z\approx 4$. The appearance of nonzero contact forces for cellular aggregates already at $Z\approx 2$ is a result of slow relaxation. If two membranes collide they are very slowly pushed away from each other (this is seen, e.g., in Fig. 1 for $Pl=10$).

When Z approaches 4 the packings already enter the dense state. In the dilute region all the membrane areas are similar. In the dense region the membrane areas (a) fluctuate. The fluctuations are Gaussian, which is demonstrated in Fig. 2(d). The average membrane area is $\langle a\rangle \equiv \Sigma N a_i/L^2 \approx 0.91$ with a standard deviation of 0.15. This distribution is not particularly broad, which suggest that it might be feasible to describe the forces on the membranes by an estimation of the average.

Equation (3) can be used as an approximation of the total force on a membrane as a function of pressure P and effective radius $r_i=\sqrt{a_i/\pi}$. However, the total force on a membrane does not compare easily with simulation results because of boundary effects. The average of the contact forces on a membrane is much less sensitive in this respect. Figures 3(a) and 3(b) show $F_a(P,r)=f(P,r)/Z(P)$ compared with the average of the contact forces recorded in the simulations, F_s, (i.e., averaged over $[F_a,F_a+\delta f]$ using the results of several runs). It is obvious that $F_a(P,r)$ describes very well the average of the contact forces. This means that the only missing piece for a full description of the distribution of contact forces are the fluctuations of F_s.

At the jamming transition the fluctuations of the contact forces in granular media have a characteristic distribution [9–11,14,15]. The characteristic distribution reaches a maximum at a small force and decays exponentially for large forces. In Fig. 3(c) we compare the contact force fluctuations $[f/f^* \equiv f/F_a(P,r)]$ at $Z(P)\approx 2$ for both frictional and frictionless packings. The two distributions are approximately similar and have the characteristic shape of granular packings at the jamming transition.

In Fig. 3(d) the same distributions are displayed at $Z(P)\approx 4.5$. Here the force distribution for frictional packings is described by an exponential function, $\exp(-f/f*)$, while the distribution for frictionless particles is well approximated by a Gaussian (in the latter case it is also possible that the decay of the probability distribution for large forces is linear exponential $[\exp(-f/f*)]$ as in Ref. [15] instead of Gaussian $\{\exp[-(f/f*)^2]\}$.

The most important result here is the dramatic difference in the development of the contact force distributions in the small $(-f/f*)$ limit for zero and high friction. While the fraction of small contact forces have clearly decreased for zero friction packings it has actually increased for high friction packings. The (almost) Gaussian curve for frictionless particles at high pressures implies that the force chains have been relaxed. The exponential force fluctuations at high Z for type (I) particles (high friction) means that the force chain network is persistent and that the force distribution is "frozen" in a state of maximum entropy (this can be derived analogously to the derivation of the Maxwell-Boltzmann distribution of kinetic energy in an ideal gas). This is a result which may have important biological implications as will be discussed below.

A force chain network for different pressures (P) is displayed in Fig. 4 for the type (I) packing. This figure can be compared to, e.g., a similar figure in Ref. [7]. The displayed

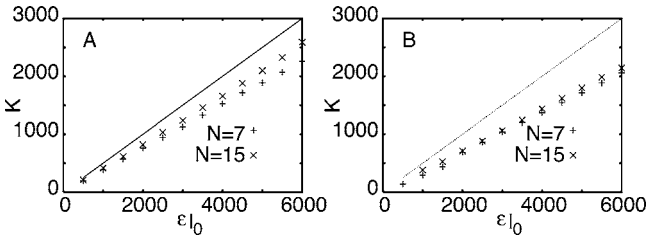

FIG. 5. (a) The bulk modulus K as a function of membrane stiffness, ϵl_0, for frictionless membranes. (b) Same as in (a) for frictional membranes. Simulations results for $N=7,15$ are displayed.

contact forces are here the sum of all forces between mass points of two membranes in contact in opposite to the single contact normal forces in Ref. [7]. The force chains in Fig. 4 thus include both normal and tangential forces, but a force chain network reminiscent of the those found in solid grain packings is nevertheless observed.

Next we turn to the effective stiffness of a dense packing of membranes. The bulk stiffness K is defined by

$$1/K = -\frac{1}{V}\frac{dV}{dP}, \tag{4}$$

where $V=L^2$. To obtain K, dV is defined as $dV=-4\delta L$. dP/dr can be determined from Eq. (3) by using $dP=df/(2\pi r)$ and $dr=2\delta r/L$. This gives the bulk modulus $K=\epsilon l_0/2r_0$. A corresponding estimate of the shear modulus of a packing of membranes gives zero because shearing involves no volume change for the membranes. This was also checked by simulations. Notice that cellular aggregates have no force corresponding to surface tension which gives a nonzero shear modulus in dry foams. The estimate for K is compared to simulation results of type (I) membranes (high friction) in Fig. 5(a) and for type (II) (freely sliding) membranes in Fig. 5(b). In both cases K is a fairly linear function of ϵl_0 ($r_0=1$). For frictionless particles the proportionality factor is somewhat smaller than $1/2$ but approaches this value as N is increased. For frictional membranes the proportionality factor seems to be about 0.37, which means that friction between membranes decreases bulk stiffness. This is not surprising since frictional membranes are interlocked via contacts and not all of the pressure contribute to pushing on the walls.

In summary, we have investigated dense packings of inflated membranes for two cases of friction between membranes: zero and high. The porosity at low coverage, the force on the confining box at high coverage, the average of the contact forces between membranes, the average bulk stiffness, and the average shear stiffness of packings can all be derived from the free energy, and they are all reasonably similar for both friction cases. A qualitative difference arise in the fluctuations of the contact forces. A frictionless packing is relaxed when coverage is increased, while the force chain skeleton formed at the jamming transition persist to high coverage for frictional packings.

We finish by discussing the biological implications of our results. From a life science point of view the most interesting results are in Figs. 3(c) and 3(d). Intuitively, one would think aggregates of living cells be rather relaxed with not much internal tension. That suggests that the osmotic pressure within cells induces a Gaussian pressure distribution on the cell walls in contact. That means that if the osmotic pressure was high (i.e., excess of salt in the cells) there would be a high pressure on *all* cell membrane contacts in the aggregate. That would effectively hinder the diffusion of large molecules. Such an effect could also hinder the penetration of chemotherapy drugs in tumours [2], harm the development of embryo [16], or cause a plant to suffer from a change in salinity [3,4]. As an opposite, if there would be a small fraction of frustrations in the aggregate [0.1–0.25 is enough for percolation in three-dimensional (3D) structures], there would always be a number of cell membrane contacts that never experience any pressure. Thus, some paths would remain always open for solute penetration even at a high osmotic pressure (cf. Fig. 4).

This work has been supported by the Academy of Finland and the Finnish Academy of Science and Letters.

[1] T. Hayashi and R. W. Carthew, Nature (London) **431**, 647 (2004).
[2] P. Carmeliet and R. K. Jain, Nature (London) **407**, 249 (2000).
[3] E. Hose, D. T. Clarkson, E. Steudle, L. Schreiber, and W. Hartung, J. Exp. Bot. **52**, 2245 (2001).
[4] M. A. Zwieniecki, P. J. Melcher, and M. N. Holbrook, Science **291**, 1059 (2001).
[5] *Jamming and Rheology*, edited by A. J. Liu and S. R. Nagel (Taylor & Francis, New York, 2001).
[6] C. Liu, S. R. Nagel, D. A. Schecter, S. N. Coppersmith, S. Majumdar, O. Narayan, and J. P. Witten, Science **269**, 513 (1995).
[7] F. Radjai, M. Jean, J.-J. Moreau, and S. Roux, Phys. Rev. Lett. **77**, 274 (1996).
[8] C. F. Moukarzel, Phys. Rev. Lett. **81**, 1634 (1998).
[9] C. S. O'Hern, S. A. Langer, A. J. Liu, and S. R. Nagel, Phys. Rev. Lett. **88**, 075507 (2002).
[10] R. C. Hidalgo, C. U. Grosse, F. Kun, H. W. Reinhardt, and H. J. Herrmann, Phys. Rev. Lett. **89**, 205501 (2002).
[11] H. A. Makse, D. L. Johnson, and L. M. Schwartz, Phys. Rev. Lett. **84**, 4160 (2000).
[12] L. D. Landau and E. M. Lifshitz, *Theory of Elasticity*, Course of Theoretical Physics Vol. 7, 3rd ed. (Pergamon Press, Oxford, 1986).
[13] J. A. Åström, M. Latva-Kokko, and J. Timonen, Phys. Rev. E **67**, 016103 (2003).
[14] M. L. Nguyen and S. N. Coppersmith, Phys. Rev. E **62**, 5248 (2000).
[15] J. M. Erikson, N. W. Mueggenburg, H. M. Jaeger, and S. R. Nagel, Phys. Rev. E **66**, 040301(R) (2002).
[16] A. J. Zhu and M. P. Scott, Genes Dev. **18**, 2985 (2004).
[17] See EPAPS Document No. E-PLEEE8-73-032606 for an animation of a packing inflation. For more information on EPAPS, see http://www.aip.org/pubservs/epaps.html.